OPEN ACCESS

Environment & Ecology ARTICLE

Leaf senescence as a natural "free radical factory" producing environmentally persistent free radicals

Hongke Feng,[1] Xingzhi Jin,[1] Fuxuan Ren,[1] Peilin Yang,[1] Junjie Wang,[1] Xiaohu Zhang,[1] Yi Yang,[1] Jianwei Li,[4] Hao Chen,[1] Peng Cai,[2,3,*] and Xing Ding[1,*]

*Correspondence: dingx@mail.hzau.edu.cn (X.D.); cp@mail.hzau.edu.cn (P.C.)

Received: December 17, 2025; Accepted: June 9, 2026; Published Online: June 10, 2026; https://doi.org/10.59717/j.xinn-geo.2026.100241

GRAPHICAL ABSTRACT

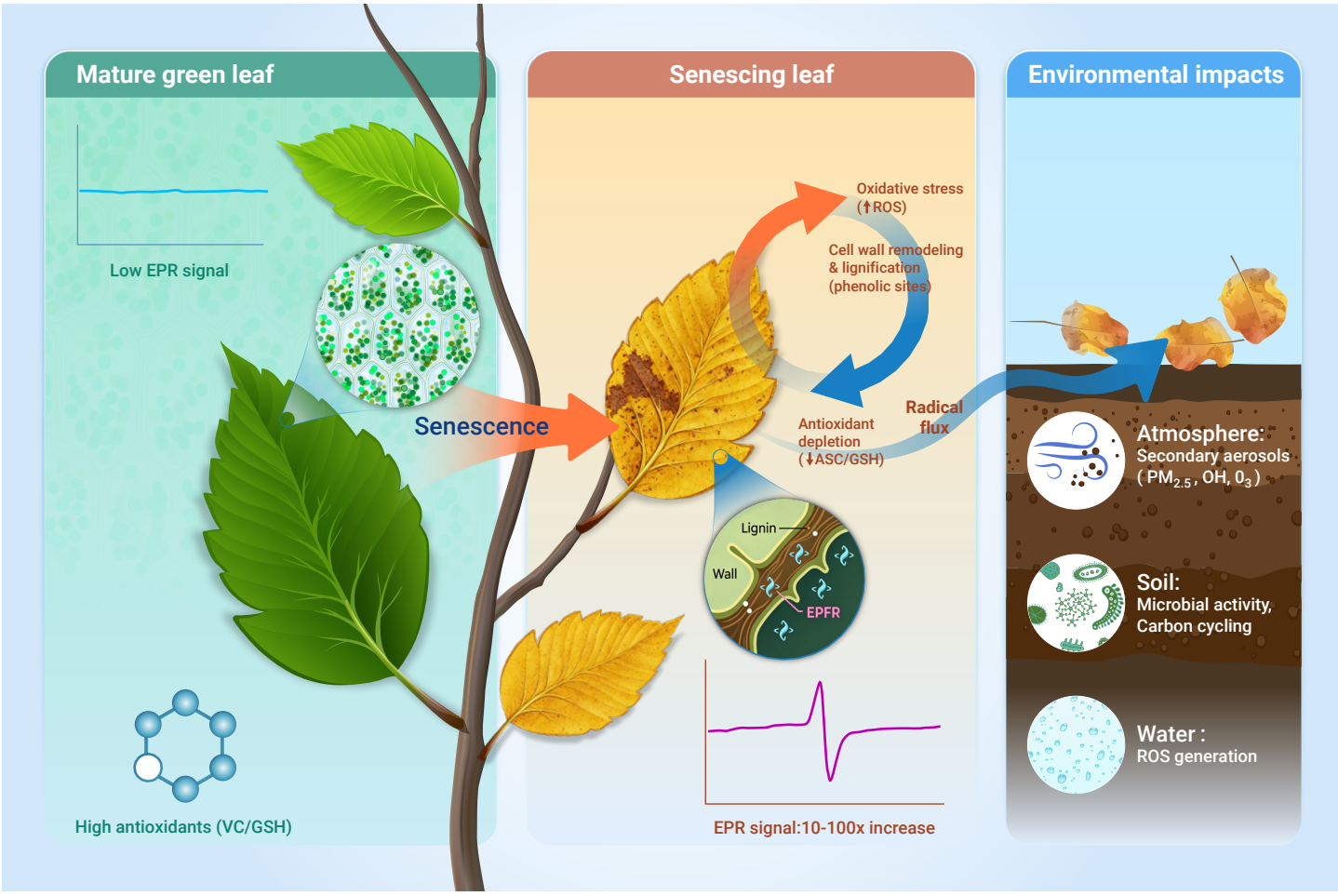

PUBLIC SUMMARY

- Leaf senescence produces environmentally persistent free radicals (EPFRs), a newly identified natural source.
- Cell wall remodeling and lignin accumulation provide phenolic sites for stabilizing EPFRs during senescence.
- Declining antioxidants and elevated oxidative stress drive EPFRs formation in senescent leaves.
- Senesced crop residues contain high levels of EPFRs, potentially impacting soil health and carbon cycling.
- The senescence program itself, not merely water loss, is the key driver of EPFRs generation.

ARTICLE Environment & Ecology

OPEN ACCESS

Leaf senescence as a natural "free radical factory" producing environmentally persistent free radicals

Hongke Feng,[1] Xingzhi Jin,[1] Fuxuan Ren,[1] Peilin Yang,[1] Junjie Wang,[1] Xiaohu Zhang,[1] Yi Yang,[1] Jianwei Li,[4] Hao Chen,[1] Peng Cai,[2,3,*] and Xing Ding[1,*]

[1]College of Chemistry, Huazhong Agricultural University, Wuhan 430070, China

[2]National Key Laboratory of Agricultural Microbiology, Huazhong Agricultural University, Wuhan 430070, China

[3]Hubei Key Laboratory of Soil Environment and Pollution Remediation, Huazhong Agricultural University, Wuhan 430070, China

[4]Macao Institute of Materials Science and Engineering (MIMSE), Faculty of Innovation Engineering, Macau University of Science and Technology, Macao SAR 999078, China

*Correspondence: dingx@mail.hzau.edu.cn (X.D.); cp@mail.hzau.edu.cn (P.C.)

Received: December 17, 2025; Accepted: June 9, 2026; Published Online: June 10, 2026; https://doi.org/10.59717/j.xinn-geo.2026.100241

Citation: Feng H., Jin X., Ren F., et al. (2026). Leaf senescence as a natural "free radical factory" producing environmentally persistent free radicals. *The Innovation Geoscience* **4**:100241.

Environmentally persistent free radicals (EPFRs) are emerging pollutants of global concern, yet their natural sources remain largely undefined. Here, we identify natural leaf senescence as a major, previously unrecognized source of EPFRs in terrestrial ecosystems. By conducting a cross-species analysis of woody and herbaceous plants, we show that EPFR formation is consistently triggered during senescence, producing markedly elevated electron paramagnetic resonance (EPR) signals compared with mature foliage. Importantly, this radical generation is driven by the senescence process itself—rather than mere water loss. Mechanistic analyses reveal that cell wall remodeling, characterized by lignin accumulation, provides phenolic-rich reaction sites for radical stabilization, while concurrent antioxidant depletion and heightened oxidative stress create a permissive redox environment. Our findings establish plant senescence as a critical biological generator of EPFRs, with implications for understanding radical fluxes in the soil–plant–atmosphere continuum and for re-evaluating the environmental impact of agricultural residue management.

INTRODUCTION

EPFRs, pollutants characterized by long-lived unpaired electrons, can migrate, transform, and accumulate continuously across various environmental media (e.g., atmosphere, soil, and water), posing long-term risks to ecosystem integrity and human health.[1-5] Current research on EPFRs has largely focused on anthropogenic formation pathways, including fossil fuel combustion, biomass pyrolysis, industrial emissions, and the secondary transformation in atmospheric particulates.[6-9] These studies have unequivocally established anthropogenic activities as major sources of EPFRs,[10-12] forming a basis for emission control strategies. In contrast, the natural origins of EPFRs remain largely unexplored, leaving a critical gap in understanding whether and how natural ecosystems contribute to the global budget of these pollutants.

This knowledge gap is particularly pronounced in terrestrial ecosystems, where the plant–soil system dominates organic carbon cycling. While free radical processes are integral to many biochemical pathways, a systematic link between plant development and EPFRs formation has yet to be established. This omission limits our ability to model the full environmental lifecycle of EPFRs. Although early sporadic studies reported electron paramagnetic resonance (EPR) signals in dried or ground plant leaves, such disruptive preparation inevitably compromises cellular integrity and moisture status, making it difficult to discern genuine endogenous EPFRs from methodological artifacts.[13] Thus, it remains unclear whether plants endogenously produce EPFRs during their life cycle, when such formation occurs, and to what extent it varies across species. This uncertainty has hindered a holistic understanding of EPFRs cycling in the environment.

We hypothesize that leaf senescence, a universal physiological process marked by water loss, cell structure disintegration, decline of antioxidant substances, and accumulation of macromolecules such as lignin,[14-18] could provide ideal conditions for EPFRs generation. For instance, decreased water content could alter the stable environment of free radicals,[19-21] while phenolic structures in components like lignin might act as precursors or stable carriers of free radicals.[22-24] However, key questions lack experimental validation: (1) is EPFRs formation a universal feature of senescence across diverse plant species? (2) what are the characteristic EPR signatures of these senescence-associated EPFRs? (3) how are EPFRs levels correlated with key physiological variables (e.g., water content, cell wall components, antioxidant indicators)?

To address these questions, we designed a cross-species study encompassing representative woody (e.g., Sycamore, Ginkgo, and bamboo) and herbaceous plants (e.g., corn, cotton, and rice) from major terrestrial and agricultural ecosystems. We systematically collected intact leaves from both growing and senescent stages, avoiding any grinding and drying that could alter their native state. Using EPR spectroscopy, we quantitatively determined EPFRs parameters (e.g., spin concentration and g-factor). In parallel, we measured a comprehensive suite of physiological and biochemical indicators including water content, cell wall components (cellulose, hemicellulose, and lignin), photosynthetic pigments, antioxidants (e.g., vitamin C, vitamin E, and polyphenols), antioxidant enzyme activities (superoxide dismutase, catalase, glutathione peroxidase), and oxidative stress markers (Malondialdehyde, oxidized glutathione). By integrating EPR data with physiological metrics, we aimed to identify the key senescence-associated processes that drive EPFRs formation. This work establishes plant senescence as a previously overlooked natural source of EPFRs, providing fundamental insights into environmental radical cycling and new perspectives for assessing the impact of plant debris in agricultural and natural ecosystems.

MATERIALS AND METHODS

Collection of plant and crop leaves

Leaves of woody plants and crops were all collected at Huazhong Agricultural University, (114.35° East longitude, 30.47° north latitude, approximately 25 meters above sea level), this area is in a subtropical monsoon humid climate. The district has an average annual temperature of 16.3°C and an average annual precipitation of 1,150 mm to 1,190 mm. Specifically, leaves of various woody plants were sampled from the same branch of the same tree (in a non-experimental area), to ensure that the properties of the leaves were as consistent as possible. For the comparison between senescent and non-senescent leaves, samples were obtained from the same leaf at different growth stages. Similarly, crop leaves were sampled from the same crop plant (in an experimental area). Consistent with the sampling strategy for woody plants, senescent and non-senescent crop leaves were also obtained by sampling the same leaf at different growth stages.

Leaf EPR measurement

First, wipe the leaves clean with a clean wet wipe, then allow the surface moisture of the leaves to air-dry for a few minutes. For each leaf, when cutting tissue samples from different areas such as the base, middle and edge, the main vein should be avoided. After thoroughly mixing the tissues, 50 milligrams should be randomly weighed for EPR determination. The specific testing method is as follows: accurately weigh 50 mg of the sample, place it in a quartz EPR tube, and conduct the test at room temperature. The detection parameters are as follows: microwave power 0.1 mW, microwave frequency 9.87 GHz, modulation frequency 100 kHz, modulation amplitude 3 g, scanning range 332-352 mT, and scanning time 60 s. The intensity of EPFRs is determined by the spin concentration, and the type is determined by the numerical range of the hyperfine coupling constant and the G-factor. To ensure the reliability of the test results, each sample is scanned in parallel

three times, and the average value is taken as the final result.

Leaf moisture content determination

The gravimetric method was used to determine the leaf water content, following the steps below: First, remove surface dust and necrotic tissues from the leaves, then cut the leaves into pieces. Weigh a dried and cooled empty crucible (recorded as m_0); weigh 10 g of the leaf sample, place it into the crucible, and record the total mass (recorded as m_1). Next, dry the crucible with the leaf sample at a constant temperature of 105°C until a constant weight is achieved; after cooling, weigh the crucible again (recorded as m_2). The leaf water content was calculated using the formula: $(m_1 - m_2)/(m_1 - m_0)\times100\%$. Each measurement was performed in 3 parallel experiments, and the average value was used as the final result.

Determination of leaf photosynthetic pigments

SPAD measurement: after powering on and self-checking, calibrate the instrument. Open the measuring clamp and perform a blank measurement until calibration success is displayed. Select healthy, undamaged, and surface-dry leaves, avoid the main vein, clamp the middle part of the leaf, and press the measurement button to read the SPAD value. Measure 3 times at different positions of the same leaf and take the average value.

Determination of cellulose, hemicellulose, and lignin

Sample Preparation: take fresh leaves, wash and dry them. Grind the material to pass through a 40-mesh sieve. Accurately weigh 1.0 g of the sample and place it in a conical flask. Add 80% ethanol and soak for 24 hours to remove soluble sugars and other impurities. Filter the mixture. Wash the residue sequentially with ethanol and distilled water. Dry at 105°C to constant weight. Record the residue mass (denoted as M1). Hemicellulose Determination: Add 100 mL of 2 mol/L hydrochloric acid to the residue. Reflux in a boiling water bath for 2.5 hours. Filter while hot. Wash the residue with hot distilled water until neutral. Dry at 105°C to constant weight (denoted as M2). Hemicellulose content = (M1 - M2) / Sample mass×100%. Cellulose determination: Transfer the residue corresponding to M2 to a conical flask. Add 100 mL of 72% sulfuric acid and let stand at 25°C for 4 hours. Dilute with distilled water to a sulfuric acid concentration of 2 mol/L. reflux in a boiling water bath for 2.5 hours, filter, wash the residue with hot distilled water until neutral, and dry at 105°C to constant weight (denoted as M3). Cellulose content = (M2 - M3) / Sample mass × 100%. Lignin determination: Place the residue corresponding to M3 into a muffle furnace, ash at 550°C for 4 hours, cool, and weigh (denoted as M4). Lignin content = (M3 - M4) / Sample mass × 100%. Perform three parallel determinations and take the average.[25]

Assay of antioxidant enzymes and antioxidant substances

Oxidized glutathione (GSSG) was determined by the DTNB colorimetric method; MDA was determined by the thiobarbituric acid (TBA)-colorimetric method; polyphenol content was determined by ultraviolet (UV) spectrophotometry; vitamin C (ascorbic acid) was determined by the 1,10-phenanthroline colorimetric method; vitamin E (tocopherol) was determined by the 1,10-phenanthroline colorimetric method; superoxide dismutase (SOD) was determined by the nitroblue tetrazolium (NBT) photoreduction method; catalase (CAT) was determined by the hydrogen peroxide (H_2O_2)-ammonium molybdate catalytic decomposition method; and glutathione peroxidase (GPx) was determined by the DTNB colorimetric method.[26]

Determination of ROS

The generation of ROS was detected using an EPR spectrometer. For the specific operation, 1 mL of sample was taken every 10 minutes, which was then drawn into a glass capillary for EPR measurement. The instrument parameters were as follows: magnetic field range of 330-345 mT, microwave frequency of 9.5 GHz, microwave power of 10 mW, and scanning time of 60 s. DMPO (100 mM) and TEMP (50 mM) were used as free radical scavengers to measure the generation of •OH, $\bullet O_2^-$, and $^1O_2$, with the same instrument parameters applied: magnetic field range of 330-345 mT, microwave frequency of 9.5 GHz, microwave power of 10 mW, and scanning time of 60 s.[27]

Detection of SOD activity, Detection of oxidized glutathione content, Detection of vitamin C content, CAT activity detection, Determination of MDA content, Detection of vitamin E content, Determination of GPX activity, Detailed experimental methods and steps are provided in the supplemental information (see Text S1-S7).

RESULTS

EPFRs are ubiquitously generated in senescent leaves

We employed electron paramagnetic resonance spectroscopy (EPR) to characterize the formation of EPFRs during leaf senescence across multiple plant species. Both qualitative (signal peaks, g-factor) and quantitative (spin concentration) analyses were performed to provide phenomenological support for subsequent investigations into the driving factors. For all tested plants, including Sycamore, Ginkgo, and corn leaf, distinct characteristic EPR signal peaks were observed in senescent leaves, whereas no appreciable signals were detected in leaves at the growing stage (Figure 1A). This result demonstrates that EPFRs generation is a universal phenomenon associated with natural leaf senescence, challenging the conventional view that EPFRs originate predominantly from anthropogenic processes or artificially dried plant materials. Quantitative analysis indicates that the spin concentration of EPFRs in senescent leaves is significantly increased. Specifically, the spin concentrations of EPFRs in senescent leaves of rice and corn reached 1.8×10^{18} spins/g and 1.3×10^{18} spins/g, respectively, while those in leaves at the growing stage were nearly negligible (Figure 1B). This indicates that senescence significantly drives the massive accumulation of EPFRs, suggesting that plant debris may represent a significant reservoir of EPFRs. Meanwhile, the g-values of all senescent leaves exceeded 2.004, identifying the radicals as oxygen-centered and confirming the consistency of radical types across species (Figure 1C). For subsequent mechanistic analyses, corn was selected as the representative species. The cross-species EPR data in Figure 1 confirm the universality of EPFRs formation across diverse plant taxa, while corn enables in-depth mechanistic investigation due to its well-defined senescence progression, sufficient biomass for multi-assay measurements, and its status as one of the highest-yielding crops globally—making senesced corn leaves a dominant agricultural residue with high environmental relevance.

Morphological and physicochemical changes promote a permissive environment

Scanning electron microscopy (SEM) revealed striking morphological differences between growing and senescent leaves. The epidermal cells of growing leaves are tightly arranged with continuous, smooth cuticle, preserving a stable internal environment (Figure 2A). In contrast, senescent leaves exhibited structural disintegration, featuring disordered cell arrangement, enlarged intercellular spaces, cuticle rupture, and granular deposits. This physical breakdown facilitated water loss and increased the exposure of internal tissues to air, thereby promoting contact between potential radical precursors and atmospheric oxygen.[13] The physical deterioration was accompanied by changes in surface properties and internal chemistry. The water contact angle on senescent leaves increased from 64.5° to 68.8° (Figure 2B), indicating a shift toward a more hydrophobic surface. This reduction in hydrophilicity can hinder water adsorption and retention, potentially allowing radicals to escape water-mediated quenching. Concurrently, the internal chemical microenvironment shifted, as evidenced by the increase in leaf pH during senescence (Figure S1). This alteration in acid-base balance could affect the protonation state of biomolecules and the stability of radical intermediates.

Underpinned by these physical and chemical changes, leaf water content progressively declined from 68.8% in growing leaves to just 9.7% in fully senescent leaves (Figure 2C). The significant negative correlation between leaf water dynamics and EPR signal intensity underscores the profound influence of water status on the cellular microenvironment and redox balance.[28] In hydrated, growing leaves, an intact cellular compartmentalization structure effectively sequesters free radical precursors from oxidases/metal catalysts,[29] while a functional antioxidant system rapidly scavenges transient ROS species,[30] collectively minimizing EPFRs generation. To further dissect the contribution of water loss from the senescence program, we performed a controlled drying experiment (Figures 2D-E). In growing leaves—which initially

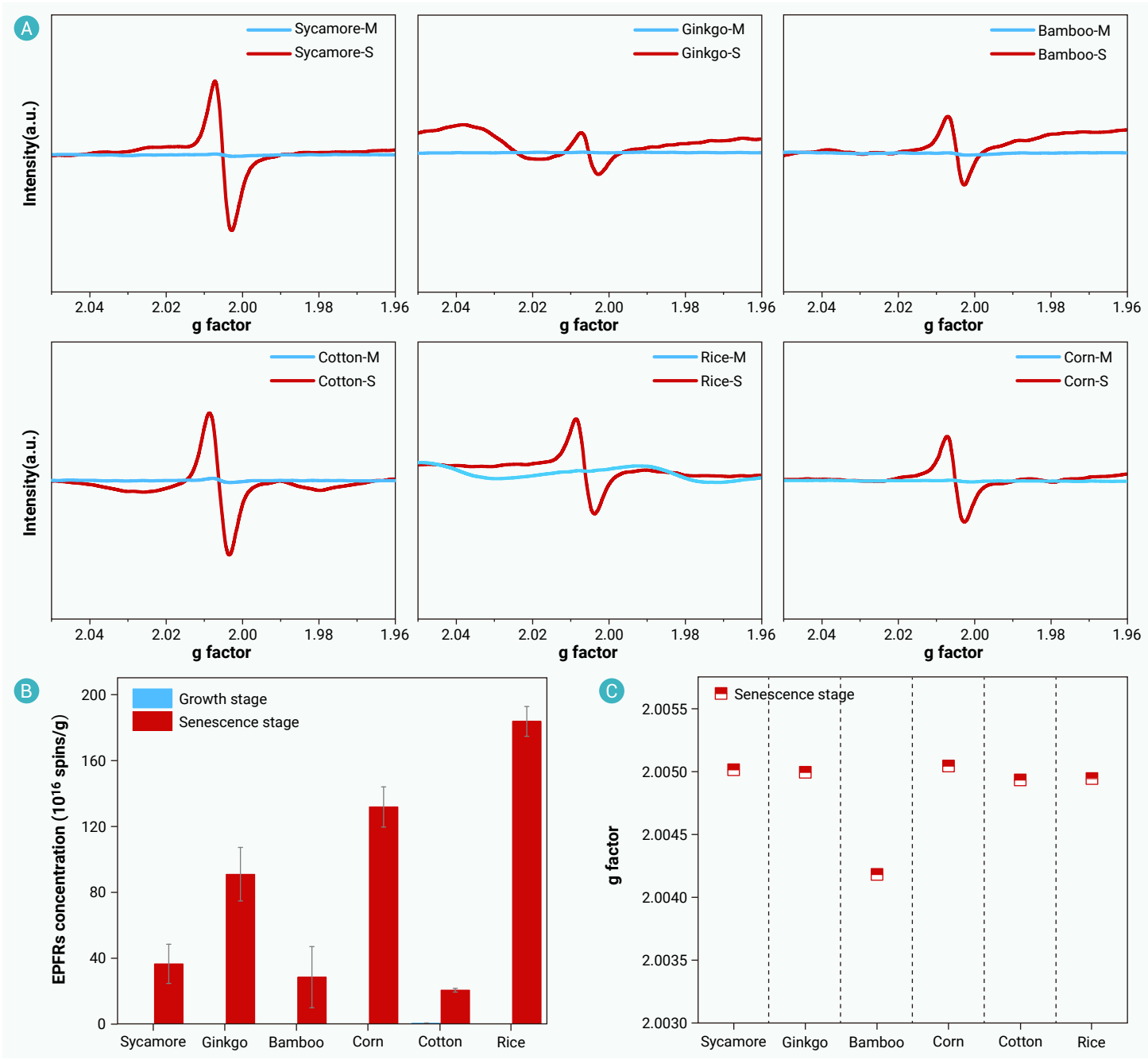

Figure 1. EPFRs are ubiquitously generated in senescent leaves (A) EPR signals of sycamore, ginkgo, bamboo, cotton, rice, and corn leaves at the growing stage and senescent stage. (B) Comparison of spin and (C) g-factor during leaf growth and senescence stages.

showed negligible EPR signals—artificial desiccation induced distinct EPR peaks (g > 2.004), marking a radical transition "from invisible to visible" (Figure S2). A similar, though less dramatic, signal enhancement upon drying was observed in semi-senescent leaves. By the senescent stage, regardless of whether the leaves are dried or not, their EPR signals are the strongest among all stages and exhibit similar peak shapes. Combined with g-factor analysis—where the g-factors of dried and original leaves at the senescent stage tend to be consistent—it can be concluded that leaves at this stage have formed a stable EPFRs generation system (Figure S3). The regulatory role of water loss weakens, and EPFRs generation relies more on the overall physiological changes induced by senescence.

Cell wall remodeling and lignin accumulation provide the material basis for EPFRs

Quantitative analysis of cell wall components during leaf senescence revealed shifts critical to EPFRs formation. The contents of cellulose and hemicellulose, the structural backbone of the cell wall polysaccharide network, declined significantly, indicating disintegration and relaxation of the cell wall architecture. This degradation not only impairs physical integrity and increases porosity but, more importantly, disrupts the encapsulating network that cross-links lignin, thereby exposing its abundant phenolic units.[31] Concurrently, the relative content of lignin, a polyphenolic polymer, showed a marked upward trend (Figure 3A). Driven by these reciprocal changes, the chemical nature of the senescent cell wall shifts from a hydrophilic, polysaccharide-dominated milieu to an interface rich in hydrophobic aromatic polymers. The accumulation of lignin forms an extensive reservoir of phenolic hydroxyl groups,[32] which under oxidative conditions can readily undergo single-electron oxidation to form stable, oxygen-centered phenoxyl radicals—consistent with the type of EPFRs (with a g-value > 2.004) identified in this study (Figure 1C).[33]

Fourier transform infrared (FTIR) spectroscopy tracked these transformations at the molecular level (Figure 3B). The progressive decrease in intensity

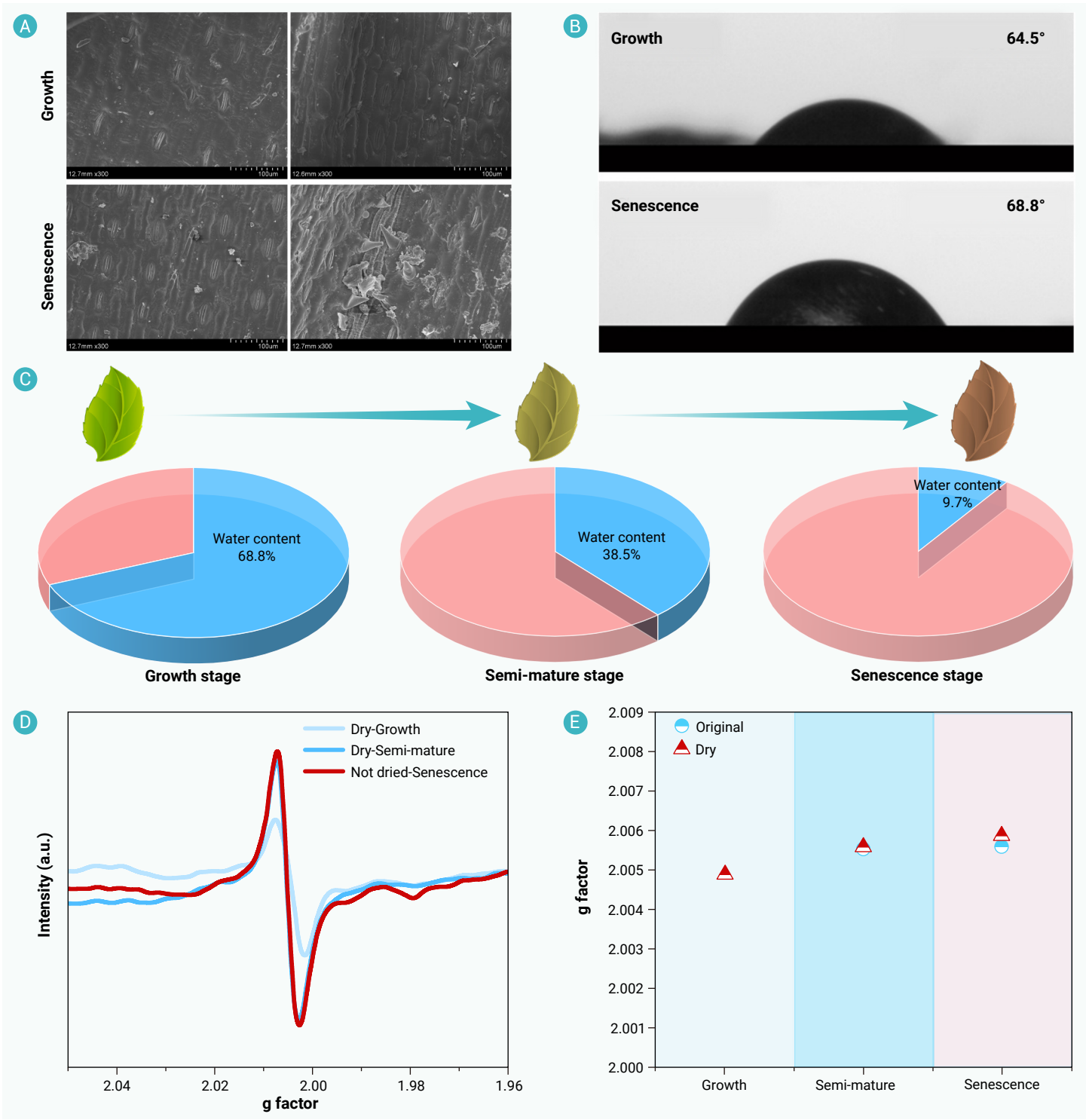

Figure 2. Morphological and physicochemical changes promote a permissive environment (A) Scanning electron microscopy (SEM) images of leaves at different growth stages. (B) Changes in water contact angle of leaves at different growth stages. (C) Changes in water content of leaves at different growth stages. (D) Comparison of the Drying Growth Stage, Drying Senescence stage, and Non-Drying Senescence stage. (E) Changes in g-factor of leaves at different growth stages after water removal compared with the original samples.

of C-O-C and C-O-H vibration bands (1,000–1,300 cm^{-1}), characteristic of carbohydrate structures, from the growing to the senescent stage, confirms the disintegration of the polysaccharide network. A notable biphasic pattern was observed for key oxidative and aromatic structures. The C=O stretching vibration around 1,700 cm^{-1} (potentially derived from -COOH or $-COO^-$ groups) and the aromatic C=C skeletal vibration bands 1,600 cm^{-1} and 1,515 cm^{-1} initially decrease from the growing to the semi-senescent stage, then increase significantly upon full senescence. Notably, lignin content increased continuously throughout senescence (Figure 3A), whereas the aromatic C=C vibration bands (1,600 cm^{-1} and 1,515 cm^{-1}) decreased initially then increased at full senescence. This late-stage rise aligns with progressive lignin accumulation under polysaccharide degradation. The resulting dense aromatic structures not only act as free radical precursors but also form a hydrophobic microenvironment that greatly facilitates the long-term stable existence of EPFRs by preventing their quenching by water molecules. Together, they construct a solid material basis for senescent leaves to function as a "free radical factory".

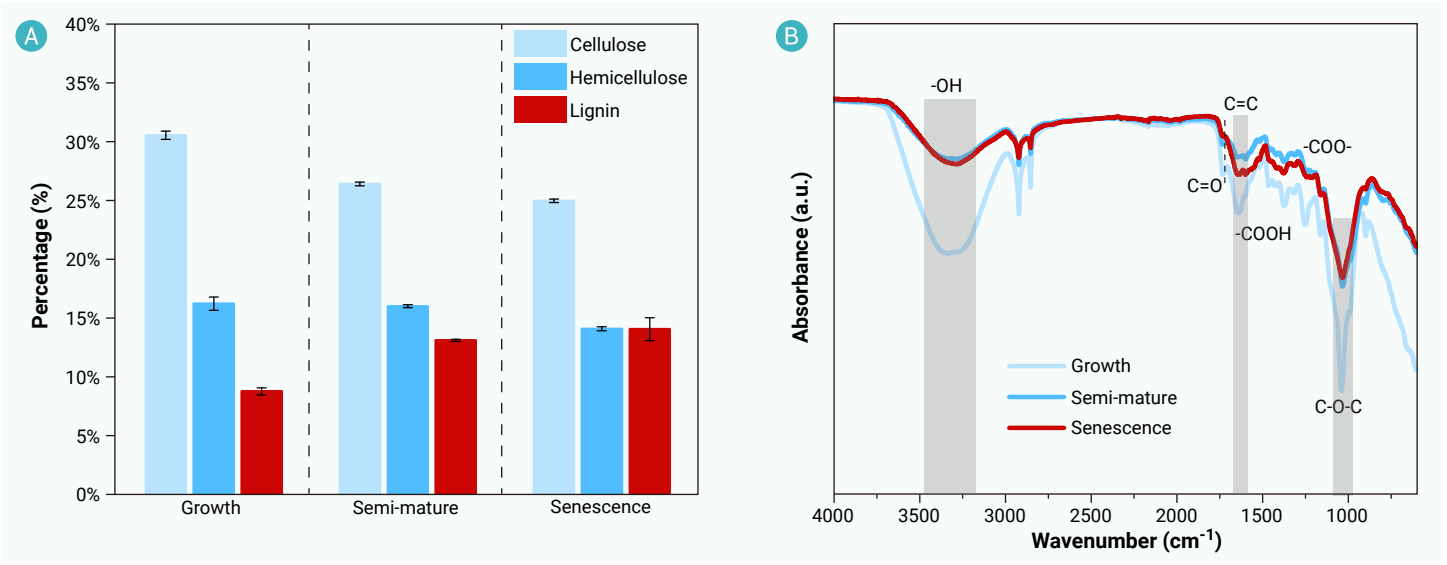

Figure 3. Cell wall remodeling and lignin accumulation provide the material basis for EPFRs (A) Changes in cellulose, hemicellulose, and lignin contents of leaves at different growth stages. (B) Comparison of infrared spectra of leaves at different growth stages.

Collapse of the antioxidant system and elevated oxidative stress drive EPFRs formation

The generation of EPFRs was further linked to the systematic decline of the antioxidant system and a surge in oxidative stress. The degradation of photosynthetic pigments, including chlorophyll and carotenoids (Figure S4), erased an inherent source of radical scavenging activity, creating an initial "scavenging gap" that permitted early radical accumulation.[34] During the transition from growth to senescence in corn, the activities of key antioxidant enzymes, superoxide dismutase (SOD), catalase (CAT), and glutathione peroxidase (GPX) displayed varied responses. While certain enzymes, including CAT and GPX, maintained or even elevated their activity (Figures 4A-C), statistical significance analysis indicated that this compensatory response was insufficient to neutralize the continuously generated free radicals. Radar charts reveal that the distribution of antioxidant substances such as vitamin C (VC) and vitamin E (VE) differs across growth stages (Figure 4D). These antioxidants are relatively abundant in the growing stage but decrease in the senescent stage. The significant decrease in polyphenol content is likely linked to their conversion into EPFRs, as these compounds can be oxidized into persistent, oxygen-centered radicals, which coincides with the marked increase in EPFRs spin concentration observed during senescence (Figure 4E).[35,36] Antioxidant enzymes and antioxidant substances collectively constitute the plant's antioxidant defense system; a reduction in their activity or content impairs the capacity for free radical scavenging. The combined decline of enzymatic and non-enzymatic antioxidant defenses during leaf senescence progressively weakened the plant's capacity to effectively scavenge metabolic free radicals. This leads to the accumulation of reactive species, thereby promoting the formation and stabilization of EPFRs.

The accumulation of oxidative stress markers and ROS provides a direct material basis for EPFRs generation. We observed a significant increase in malondialdehyde (MDA), a marker of membrane lipid peroxidation, and oxidized glutathione (GSSG), indicative of a shifted intracellular redox state in,[37] in senescent leaves (Figure 5).

These changes reflect a state of intense oxidative stress, wherein membrane structure damage and a pro-oxidant microenvironment collectively favor EPFRs formation. Direct EPR detection of ROS further confirmed an explosive accumulation of ROS radicals during senescence (Figure S5). Compared to growing leaves, senescent leaves show markedly enhanced signals from hydroxyl radicals (•OH) and superoxide anions ($\bullet O_2^-$) trapped by DMPO, along with a pronounced increase in singlet oxygen ($^1O_2$) trapped by TEMP. These results align with the decline in non-enzymatic antioxidants and the rise in MDA and GSSG, together providing multiple lines of evidence that senescent leaves enter a state of pronounced oxidative stress conducive to EPFRs stabilization. To further clarify the molecular linkage between this pro-oxidant state and EPFR formation: the accumulated ROS, particularly hydroxyl radicals (•OH) with high oxidation potential, can directly trigger the single-electron oxidation of phenolic hydroxyl groups on lignin polymers. This reaction generates resonance-stabilized phenoxyl radicals, which correspond precisely to the oxygen-centered EPFRs (g-factor > 2.004) detected in our study. Concurrently, the significant decline in non-enzymatic antioxidants (VC, VE, and polyphenols) during senescence (Figures 4D-E) eliminates the primary "braking system" for radical scavenging. The depletion of these antioxidants, which normally terminate radical chain reactions by donating hydrogen atoms, creates a permissive redox environment where ROS can persistently attack substrates like lignin without effective quenching. Thus, the collapse of the antioxidant system does not directly supply EPFRs precursors but rather enables the shift from a reducing to an oxidizing imbalance, allowing ROS-driven EPFRs formation to proceed unabated.

Correlation analysis integrates the synergistic drivers of EPFRs generation

A correlation heatmap unified the observed physiological changes with EPFRs levels, providing a systemic view of their interactions (Figure 6). EPFRs showed a significant positive correlation with factors like water content, pH value, and lignin, indicating that these variables collectively establish a suitable physicochemical microenvironment and provide key substrates for the EPFRs formation and stabilization. Conversely, the significant negative correlation with antioxidant indicators such as SOD and VC indicates that the decline of the radical-scavenging system is a critical permissive factor for EPFRs accumulation. Significant associations were also observed with other cell wall components (e.g., cellulose, hemicellulose), metabolites such as carotenoids and polyphenols, suggesting that broader senescence-driven physiological remodeling indirectly promotes EPFRs generation by altering the cellular redox state.

We integrated these interactions into a coherent pathway depicting the transition from growing to senescent leaves (Figure 7). Senescence initiates water loss, chlorophyll degradation, and a decline in antioxidants (e.g., VC, VE), while simultaneously driving lignin accumulation and elevating oxidative stress markers (e.g., ROS, MDA, GSSG). The synergy of these processes culminates in significant EPFRs generation. This model visually encapsulates how multiple factors converge to promote EPFRs formation, establishing senescence as the central trigger of a "free radical factory" in plants (Figure 7).

DISCUSSION

This work establishes natural leaf senescence as a major, previously overlooked source of EPFRs in terrestrial ecosystems, thereby providing a critical advancement in understanding the global cycle of these pollutants. While previous studies have predominantly attributed EPFRs formation to anthro-

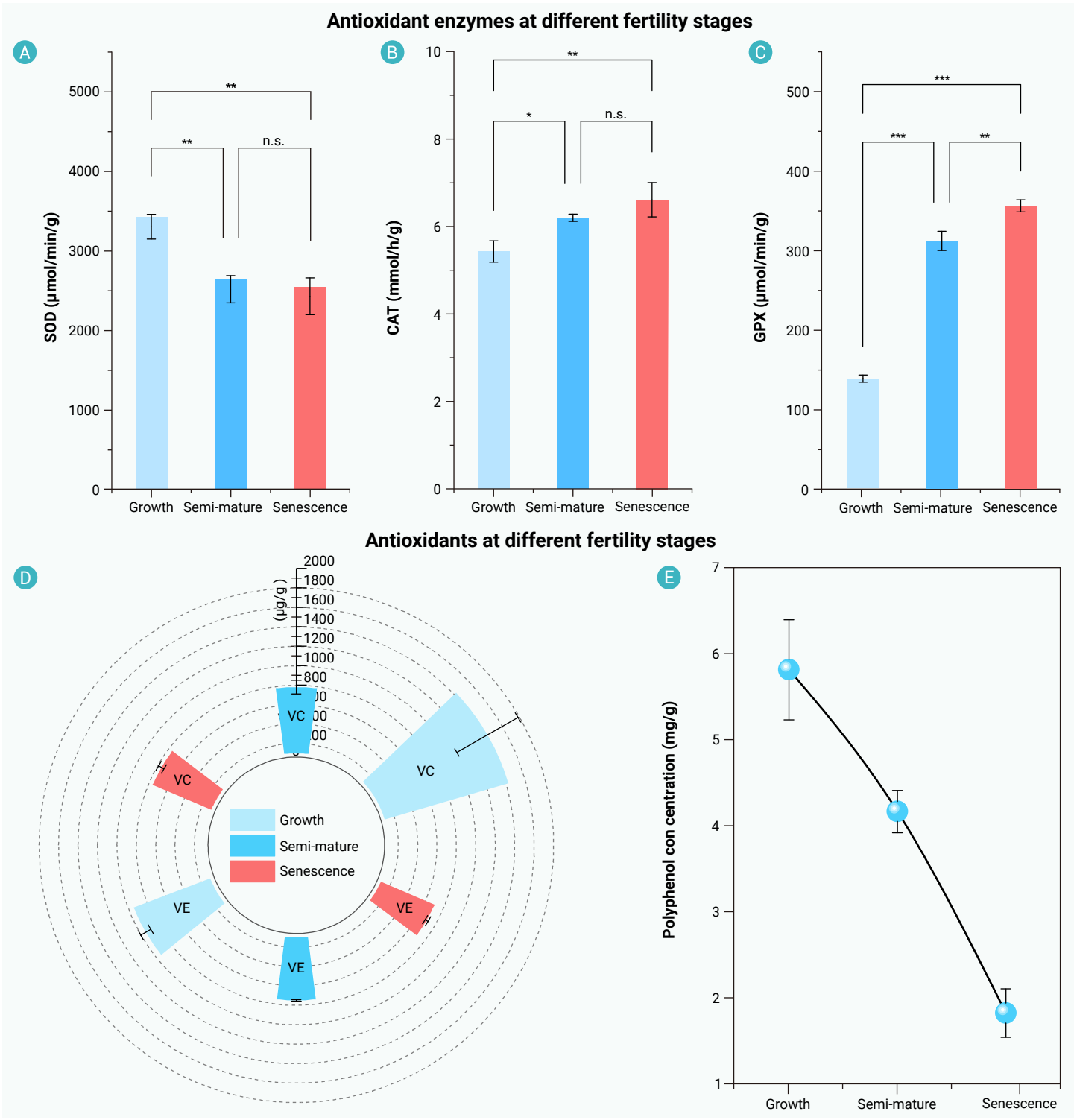

Figure 4. Collapse of the antioxidant system and elevated oxidative stress drive EPFR formation (A) Changes in superoxide dismutase (SOD) activity, (B) catalase (CAT) activity, (C) glutathione peroxidase (GPX) activity of leaves at different growth stages. (D) Changes in vitamin C (VC) and vitamin E (VE) contents of leaves at different growth stages. (E) Changes in polyphenol content of leaves at different growth stages.

pogenic processes such as fossil fuel combustion, biomass pyrolysis, and industrial emissions,[38] evidence for natural generation pathways within ecosystems has remained scarce. By conducting a cross-species investigation of woody and herbaceous plants, we consistently detected distinct EPFRs-specific EPR signals in senescent leaves—signals that were absent or minimal in growing leaves. The significant increase in spin concentration during senescence, indicative of altered radical character or chemical environment, demonstrates that EPFRs generation is a universal phenomenon in senescing plants. This finding substantially expands the paradigm of EPFRs origins beyond human activity.

The core mechanism underlying EPFRs formation during senescence involves the synergy of multiple physiological processes, with the senescence program itself—not merely water loss—serving as the principal driver. Although water loss contributed to EPFRs generation at the semi-senescent stage, fully senescent leaves maintained the strongest and most stable EPFRs signals even after eliminating variations in water content. This clarifies that water acts as a stage-specific modulator rather than a deterministic factor. Further analysis revealed that cell wall remodeling (marked by lignin

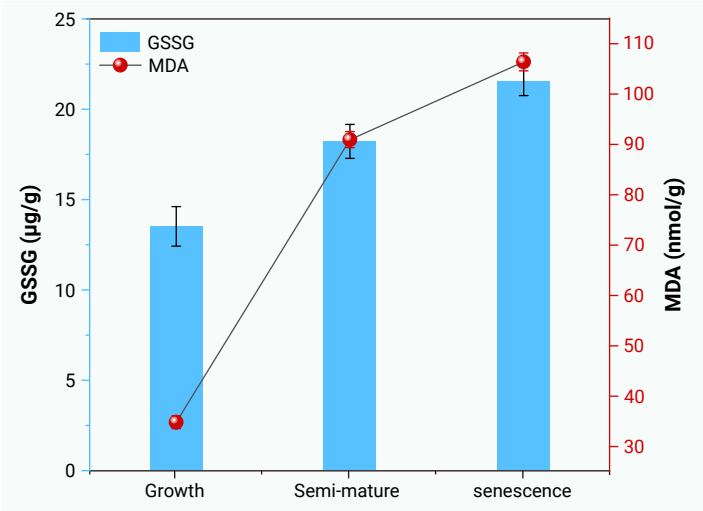

Figure 5. Changes in antioxidant markers during leaf development Comparison of malondialdehyde (MDA) and oxidized glutathione (GSSG) contents in leaves at different growth stages.

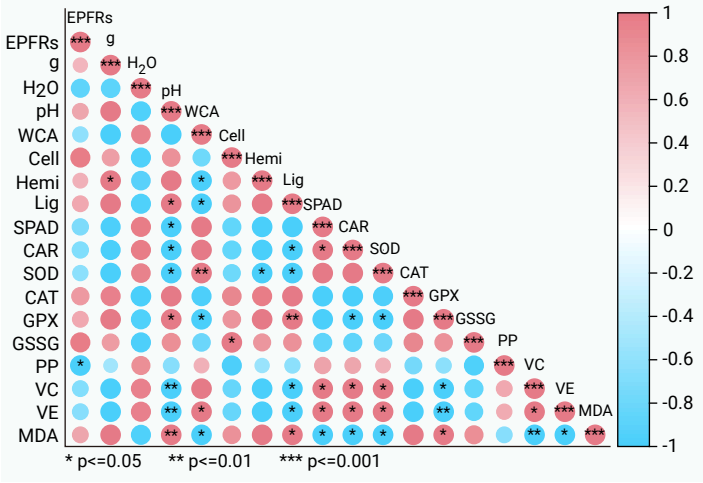

Figure 6. Correlation analysis integrates the synergistic drivers of EPFR generation.

accumulation) supplied phenolic-rich sites for radical stabilization. Lignin, due to its chemical properties and the temporal correlation with free radical accumulation, is the main structural scaffold for stabilizing EPFRs. However, the contributions of other aging-related components (such as degraded proteins or humus-like substances) cannot be completely ruled out. In the future, research needs to be conducted through isotope labeling or component-specific radical quenching techniques to quantify their relative contributions. The collapse of the antioxidant system, reflected in the depletion of VC, VE, and polyphenols, and the compromised activity of enzymes such as SOD, led to redox dysregulation. The intensified oxidative stress, evidenced by the accumulation of ROS, MDA, and GSSG, created a permissive chemical environment for EPFRs persistence. Moreover, by using intact leaves and avoiding disruptive pretreatments such as grinding or drying, this study prevented artifacts from artificial radical generation, thereby resolving earlier controversies regarding EPFRs detection in plant tissues and enhancing the ecological validity of the findings.

The findings of this study extend to both ecological understanding and agricultural practice. In agricultural ecosystems, crop residues (e.g., senescent leaves of corn and rice) are the primary source of soil biomass input. With measured EPFRs spin concentrations reaching 1.3–1.8 × 10^{18} spins/g, these materials could potentially serve as a source of EPFRs upon incorporation into soils, and previous studies have shown that EPFRs at comparable concentrations can influence microbial communities and element cycling in environmental matrices.[39,40] These results provide foundational data for assessing the environmental risk of agricultural waste. Furthermore, the

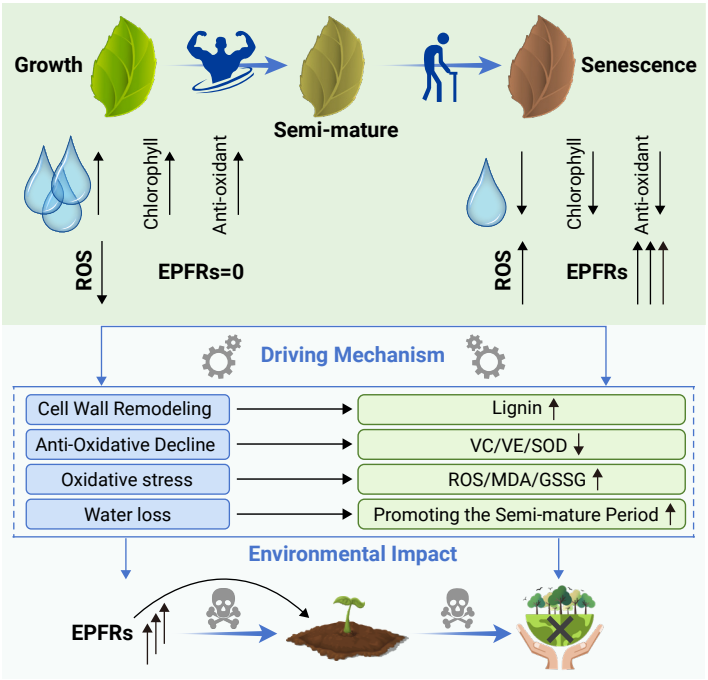

Figure 7. A coherent pathway depicting the transition from growing to senescent leaves.

contribution of plant senescence to the radical load in terrestrial ecosystems has hitherto been absent from environmental models. By identifying this pathway, our study enables more accurate simulation of EPFRs fate and transport across the soil–plant–atmosphere system and refines frameworks for ecological risk assessment.

We acknowledge that all leaf samples were collected from a single university campus, and while our paired sampling design (green vs. senescent leaves from the same plant) effectively controls for local soil, microclimate, and atmospheric variables when comparing senescence stages, the absolute EPFRs levels and their environmental relevance may vary across different geographic settings. Future multi-site investigations are therefore needed to assess the influence of broader environmental factors on senescence-driven EPFRs formation. Despite these insights, several research directions warrant further investigation. First, the specific role of lignin-derived functional groups—such as phenolic hydroxyl moieties—in EPFRs formation should be elucidated to clarify precursor transformation pathways. Second, agricultural strategies for mitigating EPFRs emissions should be explored, including optimized crop residue management (e.g., composting or mechanical incorporation) and modulation of senescence timing. Finally, in intensive monoculture systems, synchronous leaf senescence may lead to pulsed EPFRs release, which could exacerbate soil oxidative stress and alter microbial functionality, potentially influencing soil health and carbon sequestration capacity. Addressing these questions will be essential for developing a full lifecycle perspective of biogenic radicals in managed and natural ecosystems.

REFERENCES

1. Xu Y. L., Lu X. F., Su G. J., et al. (2023). Scientific and regulatory challenges of environmentally persistent free radicals: From formation theory to risk prevention strategies. *J. Hazard. Mater.* **456**:131674. DOI:10.1016/j.jhazmat.2023.131674
2. Wang X. Y., Liu H. J., Xue Y. G., et al. (2024). Formation of environmentally persistent free radicals and their risks for human health: A review. *Environ. Chem. Lett.* **22**:1327–1343. DOI:10.1007/s10311-024-01701-x
3. Xie L. Y., Zhu K. C., Chen N., et al. (2024). A critical review of an environmental risk substance induced by aging microplastics: Insights into environmentally persistent free radicals. *Environ. Sci. Technol.* **58**:22502–22518. DOI:10.1021/acs.est.4c09107
4. Zhao X. Q., Tang L., Zhang S., et al. (2024). Formation and biotoxicity of environmentally persistent free radicals in steelworks soil under thermal treatment. *J. Hazard. Mater.* **467**:133697.DOI:10.1016/j.jhazmat.2024.133697
5. Zhang Y. Q., Huang W. X., Wang H. C., et al. (2025). Environmentally persistent free radical emissions from indoor urning of pelletized biofuels. *Environ. Sci. Technol.*

59:5661–5671. DOI:10.1021/acs.est.4c14542
6. Zhao S., Gao P., Miao D., et al. (2019). Formation and evolution of solvent-extracted and nonextractable environmentally persistent free radicals in fly ash of municipal solid waste incinerators. *Environ. Sci. Technol.* **53**:10120–10130. DOI:10.1021/acs.est.9b03453
7. Hu Y. J., Zhang B. N., Guo Q. Q., et al. (2022). Characterization into environmentally persistent free radicals formed in incineration fly ash and pyrolysis biochar of sewage sludge and biomass. *J. Clean. Prod.* **373**:133666. DOI:10.1016/j.jclepro.2022.133666
8. Zhao X. Q., Cheng P. F., Borch T., et al. (2022). Humidity induces the formation of radicals and enhances photodegradation of chlorinated-PAHs on Fe(III)-montmorillonite. *J. Hazard. Mater.* **423**:127210. DOI:10.1016/j.jhazmat.2021.127210
9. Shah S., Chen J., Saleem A. R., et al. (2025). Source-oriented pollution characteristics and decay kinetics of environmentally persistent free radicals in PM2.5 and PM10. *J. Hazard. Mater.* **495**:139074. DOI:10.1016/j.jhazmat.2025.139074
10. Ai J., Qin W. H., Chen J., et al. (2023). Pollution characteristics and light-driven evolution of environmentally persistent free radicals in PM2.5 in two typical northern cities of China. *J. Hazard. Mater.* **454**:131466. DOI:10.1016/j.jhazmat.2023.131466
11. Li K., Chen Z. L., Hao W. Q., et al. (2024). Differential inhibition of tire wear particles on sludge dewatering by aging modes. *J. Hazard. Mater.* **480**:136214. DOI:10.1016/j.jhazmat.2024.136214
12. Zhou H. H., Wang X., Sun H., et al. (2025). Soil heterogeneity influences the biotoxicity of photoaged tire wear particles in Eisenia fetida: A comparative assessment. *J. Hazard. Mater.* **496**:139474. DOI:10.1016/j.jhazmat.2025.139474
13. Vejerano E. P. and Ahn J. (2023). Leaves are a source of biogenic persistent free radicals. *Environ. Sci. Technol. Lett.* **10**:662–667. DOI:10.1021/acs.estlett.3c00277
14. Sakuraba Y., Jeong J., Kang M. Y., et al. (2014). Phytochrome-interacting transcription factors PIF4 and PIF5 induce leaf senescence in Arabidopsis. *Nat. Commun.* **5**:4636. DOI:10.1038/ncomms5636
15. Kräutler B. (2016). Breakdown of chlorophyll in higher plantsphyllobilins as abundant, yet hardly visible signs of ripening, senescence, and cell eeath. *Angew. Chem. Int.* **55**:4882–4907. DOI:10.1002/anie.201508928
16. Woo H. R., Masclaux-Daubresse C. and Lim P. O. (2018). Plant senescence: How plants know when and how to die. *J. Exp. Bot.* **69**:715–718. DOI:10.1093/jxb/ery011
17. Jia M., Liu X. Y., Xue H., et al. (2019). Noncanonical ATG8-ABS3 interaction controls senescence in plants. *Nat. Plants.* **5**:212–224. DOI:10.1038/s41477-018-0348-x
18. Xue F., Li X., Qin L. X., et al. (2021). Anti-aging properties of phytoconstituents and phyto-nanoemulsions and their application in managing aging-related diseases. *Adv Drug Deliver Rev.* **176**:113886. DOI:10.1016/j.addr.2021.113886
19. Khachatryan L., McFerrin C. A., Hall R. W., et al. (2014). Environmentally persistent free radicals (EPFRs). 3. Free versus bound hydroxyl radicals in EPFRaqueous solutions. *Environ. Sci. Technol.* **48**:9220-9226. DOI:10.1021/es501158r
20. Yang X., Liu F. B., Yang S. Q., et al. (2024). Atmospheric evolution of environmentally persistent free radicals in the rural North China Plain: Effects on water solubility and PM2.5 oxidative potential. *Atmos. Chem. Phys.* **24**:11029-11043. DOI:10.5194/acp-24-11029-2024
21. Chen X., Alvarez P. J. J. and Masiello C. A. (2025). Environmentally persistent free radicals in biochar: Environmental context and future research needs. *Environ. Sci. Technol.* **59**:11440–11454. DOI:10.1021/acs.est.4c13603
22. Yang J., Pignatello J. J., Pan B., et al. (2017). Degradation of p-Nitrophenol by Lignin and cellulose chars: H2O2-Mediated reaction and direct reaction with the char. *Environ. Sci. Technol.* **51**:8972–8980. DOI:10.1021/acs.est.7b01087
23. Ruan X. X., Liu Y. Y., Wang G. Q., et al. (2018). Transformation of functional groups and environmentally persistent free radicals in hydrothermal carbonisation of lignin. *Bioresource Technol.* **270**:223–229. DOI:10.1016/j.biortech.2018.09.027
24. Li F. F., Chang Z. F., Khaing K., et al. (2019). Organic matter protection by kaolinite over bio-decomposition as suggested by lignin and solvent-extractable lipid molecular markers. *Sci. Total Environ.* **647**:570–576. DOI:10.1016/j.scitotenv.2018.07.456
25. Chen S. J., Xia Y. H., Zhang B. L., et al. (2021). Disassembly of lignocellulose into cellulose, hemicellulose, and lignin for preparation of porous carbon materials with enhanced performances. *J. Hazard. Mater.* **408**:124956. DOI:10.1016/j.jhazmat.2020.124956
26. Chen L., Liu Z., Yang T. H., et al. (2024). Photoaged tire wear particles leading to the oxidative damage on earthworms (eisenia fetida) by disrupting the antioxidant defense system: The definitive role of environmental free radicals. *Environ. Sci. Technol.* **58**:4500–4509. DOI:10.1021/acs.est.3c07878
27. Ni Z., Zhang C., Ma H. A., et al. (2022). Facet-dependent photo-degradation of nitro polycyclic aromatic hydrocarbons on hematite under visible light: Participation of environmentally persistent free radicals and reactive oxygen/nitrogen species. *Appl. Catal. B: Environ.* **318**:121816. DOI:10.1016/j.apcatb.2022.121816
28. Sun Y. M., Li Y. R., Wang M., et al. (2018). Redox imbalance contributed differently to membrane damage of cucumber leaves under water stress and Fusarium infection. *Plant Science* **274**:171–180. DOI:10.1016/j.plantsci.2018.05.025
29. Jezek M., Silva-Alvim F. A. L., Hills A., et al. (2021). Guard cell endomembrane Ca^{2+}-ATPases underpin a 'carbon memory' of photosynthetic assimilation that impacts on water-use efficiency. *Nat. Plants.* **7**:1301–1313. DOI:10.1038/s41477-021-00966-2
30. Cai J., Peng J., Feng J., et al. (2023). Antioxidant hepatic lipid metabolism can be promoted by orally administered inorganic nanoparticles. *Nat. Commun.* **14**:3643. DOI:10.1038/s41467-023-39423-3
31. Li T. F., Ma H., Wu S. B., et al. (2020). Effect of highly selective oxypropylation of phenolic hydroxyl groups on subsequent lignin pyrolysis: Toward the lignin valorization. *Energy Convers. Manage.* **207**:112551. DOI:10.1016/j.enconman.2020.112551
32. Liu B. W., Qi Y., Qiu X. Q., et al. (2025). Photoelectrocatalytic pathway for the preparation of power-effective aviation fuel precursors from lignin. *Adv. Funct. Mater.* **35**:2421552. DOI:10.1002/adfm.202421552
33. Silva C. D. G., Sun P. C., Barrett K., et al. (2024). Polyphenol oxidase activity on guaiacyl and syringyl lignin units. *Angew. Chem. Int.* **63**:e202409324. DOI:10.1002/anie.202409324
34. Ding N., Fei Q., Xiao D. D., et al. (2023). Highly efficient and recyclable Z-scheme heterojunction of Ag_3PO_4/g-C_3N_4 floating foam for photocatalytic inactivation of harmful algae under visible light. *Chemosphere.* **317**:137773. DOI:10.1016/j.chemosphere.2023.137773
35. Keylor M. H., Matsuura B. S., Griesser M., et al. (2016). Synthesis of resveratrol tetramers via a stereoconvergent radical equilibrium. *Science* **354**:1260–1265. DOI:10.1126/science.aaj1597
36. Li Y. J., Qin H. X., Wu D. P., et al. (2026). Natural polyphenol-promoted degradation of emerging contaminants during copper sulfide mineral oxygenation: the synergism of surface-bound radicals and singlet oxygen. *Environ. Sci. Technol.* **60**:6784–6794. DOI:10.1021/acs.est.5c16502
37. Zhang Z. M., Yang J. R., Zhou Q. L., et al. (2025). The role and mechanism of the cGAS-STING pathway-mediated ROS in apoptosis and ferroptosis induced by manganese exposure. *Redox Biology.* **85**:103761. DOI:10.1016/j.redox.2025.103761
38. Ma B., Li Y. L., Wang K., et al. (2025). In vitro physiological evaluation of metal bioaccessibility and reactive oxygen species distribution in biomass incineration lightweight mesoporous particulate matter. *J. Hazard. Mater.* **498**:139931. DOI:10.1016/j.jhazmat.2025.139931
39. Ye J. Y., Zhang Y. H., Gao Y., et al. (2025). Impacts of environmentally persistent free radicals on the denitrification toxicity of photoaged tire wear particles in estuarine sediments. *J. Hazard. Mater.* **494**:138623. DOI:10.1016/j.jhazmat.2025.138623
40. Xia W. H., Geng Z. X., Meng Z. H., et al. (2026). Photoaging-driven transformation of tire wear particles: unraveling the spatiotemporal dynamics of persistent free radicals and their phytotoxic Impact. *Environ. Sci. Technol.* **60**:996–1006. DOI:10.1021/acs.est.5c03767

FUNDING AND ACKNOWLEDGMENTS

This work was supported by the National Science Foundation for Distinguished Young Scholars of China (No. 42225706), the National Natural Science Foundation of China (Nos. 22076055, 42177281, 52372081 and 52073110), the Innovative Groups in Hubei Province (2023AFA009), the Young Top-notch Talent Training Program in Hubei Province (310-119024043), the Knowledge Innovation Program of Wuhan-Shuguang Project (No. 2022020801020226), and the Fundamental Research Funds for the Central Universities (Nos.2662025HXPY001, 2662023PY010, 2662023LXPY002 and 2662024JC013). The funders had no role in study design, data collection and analysis, decision to publish, or preparation of the manuscript.

AUTHOR CONTRIBUTIONS

F.H. K. : Methodology, Investigation, Formal analysis, Writing - Original draft. J. X. Z., R. F. X. : Investigation, Resources, Data curation. Y. P. L., W. J. J. : Resources, Data curation. Z. X. H., Y. Y. , L. J. W., C. H.: Writing - Review & editing. C. P. : Resources, Writing - Review & editing. C. P., D. X. : Conceptualization, Supervision, Writing - Review & editing, Project administration, Funding acquisition. All authors contributed to the manuscript and approved the final version.

DECLARATION OF INTERESTS

The authors declare no competing interests.

DATA AND CODE AVAILABILITY

Data are available from the corresponding author upon reasonable request.

SUPPLEMENTAL INFORMATION

It can be found online at https://doi.org/10.59717/j.xinn-geo.2026.100241.